Journal of Chromatography A, 1217 (2010) 5940–5949

Contents lists available at ScienceDirect

Journal of Chromatography A

journal homepage: www.elsevier.com/locate/chroma

Chromatographic biopanning for the selection of peptides with high specificity to Pb^{2+} from phage displayed peptide library

Rui Nian[a,1], Duck Sang Kim[b,1], Thuong Nguyen[c,1], Lihan Tan[d], Chan-Wha Kim[b], Ik-Keun Yoo[c,*], Woo-Seok Choe[a,d,**]

[a] School of Chemical Engineering, Sungkyunkwan University, Suwon 440-746, South Korea
[b] Department of Biotechnology, School of Life Sciences and Biotechnology, Korea University, Seoul 136-710, South Korea
[c] School of Chemical Engineering & Bioengineering, University of Ulsan, Ulsan 680-749, South Korea
[d] Department of Chemical and Biomolecular Engineering, National University of Singapore, Singapore 119260, Singapore

ARTICLE INFO

Article history:
Received 24 March 2010
Received in revised form 2 July 2010
Accepted 17 July 2010
Available online 23 July 2010

Keywords:
Chromatographic biopanning
Phage display
Pb^{2+}
Peptide
FPLC
Monolithic column

ABSTRACT

Toxic heavy metal pollution is a global problem occurring in air, soil as well as water. There is a need for a more cost effective, renewable remediation technique, but most importantly, for a recovery method that is selective for one specific metal of concern. Phage display technology has been used as a powerful tool in the discovery of peptides capable of exhibiting specific affinity to various metals or metal ions. However, traditional phage display is mainly conducted in batch mode, resulting in only one equilibrium state hence low-efficiency selection. It is also unable to monitor the selection process in real time mode. In this study, phage display technique was incorporated with chromatography procedure with the use of a monolithic column, facilitating multiple phage-binding equilibrium states and online monitoring of the selection process in search of affinity peptides to Pb^{2+}. In total, 17 candidate peptides were found and their specificity toward Pb^{2+} was further investigated with bead-based enzyme immunoassay (EIA). A highly specific Pb^{2+} binding peptide ThrAsnThrLeuSerAsnAsn (TNTLSNN) was obtained. Based on our knowledge, this is the first report on a new chromatographic biopanning method coupled with monolithic column for the selection of metal ion specific binding peptides. It is expected that this monolith-based chromatographic biopanning will provide a promising approach for a high throughput screening of affinity peptides cognitive of a wide range of target species.

1. Introduction

Toxic heavy metals (Co, Cd, Pb, etc.) in air, soil and water are a growing threat to the environment and human health. There are hundreds of sources of heavy metal pollution, including the coal, natural gas, paper and chlor-alkali industries [1,2]. Unlike organic pollutants, heavy metals do not decay over a long time and thus pose a different kind of challenge for remediation. Removal of heavy metals is usually accomplished through pH neutralization followed by lime-mediated precipitation, peroxide addition, reverse osmosis, and/or ion exchange [3]. However, the liming process is often associated with some disadvantages (e.g. the use of a large amount of alkaline materials, and production of secondary wastes), necessitating highly regulated and costly disposal [1,4].

Currently, plants or microorganisms are used to remove some heavy metals such as mercury [5,6]. Plants which exhibit hyper accumulation can be used to remove heavy metals from soil by concentrating them in their biomass. This is used in the treatment of mining tailings and the vegetation is then incinerated to recover the heavy metals. As an alternative to these processes many researchers have developed ligands to detect and/or precipitate heavy metals from aqueous systems. Phage display is a selection technique where a library of peptides or protein variants is expressed on the phage surface, while the genetic material encoding each variant resides inside [7–9]. This allows rapid partitioning of phage particles based on their binding affinity to a given target molecule through an in vitro selection process called panning [10]. Nowadays, phage display of combinatorial peptide libraries has become one of the standard technologies for selecting peptides cognitive of specific molecules [11]. Nevertheless, the traditional phage display techniques, relying on batch equilibrium adsorption/desorption, have significant drawbacks in terms of selection efficiency and target binding avidity. This is mainly because most of the conventional

* Corresponding author.
** Corresponding author at: School of Chemical Engineering, Sungkyunkwan University, Suwon 440-746, South Korea. Tel.: +82 31 290 7344; fax: +82 31 290 7272.
E-mail addresses: ikyoo@mail.ulsan.ac.kr (I.-K. Yoo), checws@skku.edu (W.-S. Choe).
[1] These authors equally contributed to this work.

0021-9673/$ – see front matter © 2010 Elsevier B.V. All rights reserved.
doi:10.1016/j.chroma.2010.07.048

biopanning procedures fractionate the binders from the rest in batch mode where only a single equilibrium stage separation is expected, often resulting in decreased binding efficacy of phage displayed peptides to target molecules hence repeated screening rounds. Besides, the screening processes are difficult to monitor in a real time mode, since phage particles are relatively large (e.g. 1 μm in length and less than 10 nm in diameter for M13 widely used in various biopanning procedures [12]) and thus difficult to be compatible with automated chromatography system (e.g. FPLC) typically operated with packed bed columns. Although chromatography technique has been used for phage binding test [13] following the screening process, no chromatographic procedure has been demonstrated in cooperative with phage display technique for the selection of specific affinity peptides toward target molecules.

The recent development of monolithic columns is one of the major breakthroughs in column technology. Monolithic columns are made of a single piece of porous cross-linked polymer or porous silica, thereby allowing for low column backpressure, high flow rates, faster transfer kinetics and passage of small particulates without clogging the columns. An extremely short column with large diameter channels (1500 μm) and low void volume gives an extraordinary resolution when separating proteins or other macromolecules such as DNA and viruses, while capacity remains high. The large through pore size and high porosities with a small diffusion path lead to high permeability with FPLC/HPLC instrumentation when compared to traditional columns with packed particles [14–17].

Lead, similar to heavy metal mercury, is a potent neurotoxin that accumulates in soft tissues and bone over time (especially in children) and causes systemic damage, blood and brain disorders [18,19]. Long-term exposure of lead can result in decreased functioning of the nervous system in adults. It may also cause weakness in fingers, wrists, or ankles [20]. In general, lead from wastewater can be precipitated or otherwise captured to give an insoluble form through adsorption or ion exchange [21–24]. However, the most widely used precipitation process is usually insufficient to reduce lead concentration to the level required by water quality standard [25]. The adsorption method involves the contact of the lead-containing water with a suitable adsorbent. Recently, there has been considerable interest in the use of relatively inexpensive agricultural sorbents which are capable of removing significant quantities of lead. For instance, a promising new method is to use living aquatic plants to absorb metal ion from water. It has been shown that aquatic plants are effective at separating metals from their surrounding waters [26]. This alternative process to physical and chemical based separation has been called biosorption, bioremoval, bioseparation or sometimes phytoremediation [27]. In addition, the use of biodegradable peptides as ligands to detect and/or precipitate heavy metals from aqueous systems also received much attention these days. Considering the high specificity and sensitivity of peptides (low K_d) toward target molecules, the use of peptide in sensor development is highly promising. In addition, though the usage of peptide per se on environmentally large scale for lead remediation may not be cost-effective, the use of M13 virus displaying the target cognitive peptide on the viral capsid as a biosorbent for Pb^{2+} would be economically viable [28]. The Pb^{2+} specific peptide can also be displayed as a part of surface proteins on various other microorganisms [28–31]. The biopanning in search of Pb^{2+} binders was first conducted in the conventional manner in our group, but it only gave peptides with high cross-binding affinities to other metal ions despite extensive negative selection. We thought that a more stringent negative screening strategy would be required to select peptide sequences specifically cognitive of Pb^{2+} without exhibiting cross-binding affinity to other metal ions.

In this study, a novel method based on chromatography technique for the selection of affinity peptides sequences specifically cognitive of Pb^{2+} was developed. Monolithic column with larger pore size which is sufficient for phage molecules to pass through was utilized. This chromatographic biopanning process enables multiple equilibrium stages for each round of screening, thereby greatly increasing the selection efficiency. In addition, the entire screening process can also be monitored online, providing an additional straightforward way to oversee the selection profile.

2. Experimental

2.1. Biological materials

A phage display peptide library for screening of disulfide bond constrained heptapeptide (Ph.D.—C7C™, Phage Display Peptide Library Kit, E8120S) was purchased from NEB (New England Biolabs, Beverly, MA). LB medium (10 g tryptone, 5 g yeast extract, 10 g NaCl in 1 L deionized water) supplemented with 12.5 mg/L tetracycline was used to grow *Escherichia coli* ER2738. 2 × YT medium (16 g tryptone, 10 g yeast extract, 5 g NaCl in 1 L deionized water, pH 7.0) containing 5 mM $MgCl_2$ was used in phage amplification.

2.2. Chromatographic biopanning

The chromatography system used was BioLogic DuoFlow Systems (760-2256, Bio-Rad) and the obtained data was processed with BioLogic DuoFlow Software Version 5.0. CIM® IDA monolithic column (217.3010, BIA Separations) was loaded with different types of metal ions (Pb^{2+}, Cu^{2+}, Ni^{2+}, Co^{2+} and Fe^{3+}) for chromatographic biopanning. Metal ion sources used in this study were $Pb(NO_3)_2$, $CuCl_2$, $NiCl_2$, $CoCl_2$ and $FeCl_3$, respectively. The final concentration of each metal ion solution was 50 mM. The monolithic column was loaded with 20 column volume (CV) of metal ion solution followed by 20 CV of Equilibration Buffer (0.1 M citrate–citric acid, 0.3 M NaCl, pH 5.4). All solutions were filtered through 0.22 μm filter prior to usage.

2.2.1. Pre-negative screening against uncharged monolithic column

A 100 μL sample of the phage library (~2×10^{12} virions, library complexity (unique clones) = 1.2×10^9 as claimed by NEB) was dissolved in 900 μL Equilibration Buffer and loaded to the uncharged monolithic column (1 mL bed volume, BV) in a total recycling mode. The flow rate was kept at 1 mL/min for 25 min. 2 mL of flowthrough was collected and 10 μL of which used for phage titering. Titration was conducted on agar plates supplemented with X-gal/IPTG. The rest of the phages were amplified by infecting *E. coli* ER2738 (phage library kit) in a 50 mL 2 × YT medium. The medium was incubated at 37 °C under vigorous shaking (250 rpm) for 4.5 h. The amplified phages were purified by precipitation with PEG/NaCl (20% (w/v) polyethylene glycol (PEG)-8000, 2.5 M NaCl). The amplified phages were then titered and adjusted to a desired concentration for the following positive screening. For phage titering, we used the plague forming unit assay as described by NEB manual.

2.2.2. Main biopanning (positive screening against Pb^{2+})

Three rounds of main biopanning were conducted against Pb^{2+} as a target. 100 μL of phage sample from pre-negative screening was dissolved in 900 μL Equilibration Buffer and loaded to the column pre-charged with Pb^{2+} at a flow rate of 0.5 mL/min. 50 mL of Washing Buffer 1 (0.1 M citrate–citric acid, 0.3 M NaCl, pH 5.4) was used to wash out any weakly bound phage at a flow rate of 2 mL/min. The elution was achieved by passing the column with 15 mL 1 M HCl. The flow rate was kept at

1 mL/min. The eluate (4–5 mL) was placed in a centrifugal filter device with MWCO of 100 kDa (Amicon Ultra-4 Centrifugal Filter Devices, UFC 810024, Millipore) and centrifuged at 5000 × *g* to remove the metal ions co-eluted with phage particles. The retained phages were amplified and titered. Phage solution at a desired concentration was then used in the second round of biopanning.

After the second round of positive selection, the selection power was increased by reducing the amount of immobilized Pb^{2+} in the third round positive selection. After washing the charged column with Washing Buffer 1, the column was further washed with Washing Buffer 2 (0.1 M citrate–citric acid, 0.3 M NaCl, pH 3.5) in order to wash out any metal ions unable to bind to the column at the lower pH value. The column was then re-equilibrated with Washing Buffer 1 and phage sample was applied as above. The eluate was titered and the amplified eluted phage at a desired concentration was used in the following negative selection processes.

2.2.3. Post-negative screening I (against uncharged monolithic column)

A 10 μL phage sample from the third round of positive selection was dissolved in 500 μL Equilibration Buffer and applied to uncharged monolithic column in a total recycling mode as described in the pre-negative screening. 2 mL of flowthrough was collected, amplified and used in the next round. The elution was achieved by passing the column with 1 M HCl. 4–5 mL eluate was collected and titered. After three rounds, the amplified phages at a desired concentration were used in the next post-negative screening against various other metal ions.

2.2.4. Post-negative screening II (against other metal ions)

A 10 μL phage sample from the third round of post-negative selection was dissolved in 500 μL Equilibration Buffer and applied to monolithic column (charged with different metal ions including Cu^{2+}, Ni^{2+}, Co^{2+} and Fe^{3+}) in a total recycling mode. In each step, 2 mL of flowthrough was collected and amplified for next round selection. 4–5 mL eluate was collected and titered. According to the analysis of elution profiles and the titration results, three rounds of negative selection against Cu^{2+}, three rounds against Ni^{2+}, two rounds against Co^{2+} and one round against Fe^{3+} were conducted.

2.3. DNA extraction and sequencing

Following the post-negative screening II, individual phage clones were isolated. The phage ssDNA was purified with a QIAprep M13 kit (27704, Qiagen) and used for DNA sequencing. The insert alignment was analyzed using a primer 5′-HOCCC TCA TAG TTA GCG TAA CG-3′ (S1259, NEB). 60 individual clones were sent for sequencing and 44 DNA sequences were obtained.

2.4. Affinity assay of different metal ions to IDA beads at low pH

200 μL of IDA beads (settled volume, SV) (Chelating Sepharose Fast Flow, 17-0575-01, GE Healthcare) was transferred to 1.5 mL Eppendorf tubes. The beads were washed 6 × 60 s with 1 mL water to remove entrained ethanol used for storage. 1 mL of metal ion solution in water (10 μM) was applied for 0.5 h at room temperature to charge the beads. The metal ion loaded beads were then washed six times with water followed by six times of additional washing with Washing Buffer 3 (0.1 M citrate–citric acid, 0.3 M NaCl, pH 4.0). The metal ions were then eluted with 1 M HCl and the concentration of coupled metal ions was determined by Inductively Coupled Plasma Mass Spectrometry (ICP-MS).

2.5. Bead-based enzyme immunoassay (EIA) of selected phage peptides

200 μL of IDA beads (SV) was transferred to 1.5 mL Eppendorf tubes. The beads were washed 6 × 60 s with water (1 mL each time) to remove ethanol used for storage. 1 mL of metal ion solution in water (10 μM) was applied for 0.5 h at room temperature to charge the beads. The beads were then washed six times with water followed by six times with Washing Buffer 3.

The concentration of each selected phage was adjusted to $\sim 2 \times 10^{11}$ pfu/mL and 50 μL of phage suspension in 1 mL Washing Buffer 3 was then applied to 200 μL of charged IDA beads (SV). After 1 h incubation at room temperature, the beads were washed six times with Washing Buffer 3. 1 mL of horseradish peroxidase-conjugated anti-M13 antibody (1:5000 in Washing Buffer 3) (27-9421-01, GE healthcare) was added and incubated for 1 h at room temperature. The beads were then washed for 6 × 60 s with Washing Buffer 3 containing 0.05% Tween 20. 400 μL of a substrate solution (0.05 M citric acid pH 4.0, 0.22% 2,2′-azinobis(3-ethylbenzthiazoline-6-sulfonic acid) (ABTS), 0.17% H_2O_2) was added. After 1 h incubation, the samples were centrifuged for 5 min at 10,000 × *g*. The absorbance of the supernatants at 405 nm was recorded on a microplate reader. ABTS is commonly used as a substrate together with hydrogen peroxide for a peroxidase enzyme or individually for a laccase enzyme. ABTS allows the reaction kinetics of peroxidases to be monitored.

3. Results and discussion

3.1. Characterization of the binding ability of different metal ions to IDA beads

Metallic lead is surface air-oxidized, forming a thin layer of oxide that protects it from further oxidation. The metal is resistant to sulfuric or hydrochloric acids. It does, however, dissolve in nitric acid to form $Pb(NO_3)_2$ [32]. Aqueous solutions of Pb^{2+} therefore can only be prepared by dissolving $Pb(NO_3)_2$ in distilled water and diluted to give a desired concentration. $PbCl_2$ is poorly soluble (with a solubility product constant (K_{sp}) of 1.6×10^{-5} at 25 °C) and this tends to limit the solubility of lead in saline media [32]. Lead also tends to hydrolyze and precipitate in the form of $Pb(OH)_2$ at pH above 5, therefore the selected working pH in this study was kept low. However, the low pH in chromatographic biopanning (pH 5.4, 4.0 and 3.5) may also significantly affect the binding efficiency of metal ions to IDA ligands on monolithic column used in the present study. The binding ability of different metal ions to the monolithic column at the working pH was therefore first characterized. 20 mL of metal ion solution was loaded to the monolithic column with 1 mL BV at a flow rate of 1 mL/min. The column was then washed with 60 mL Washing Buffer 1 to wash out any unbound metal ions. The elution was achieved by passing the column with 15–20 mL 1 M HCl at a flow rate of 1 mL/min. Pb^{2+} (Fig. 1), Cu^{2+} and Fe^{3+} have strong absorbance at 280 nm. Co^{2+} and Ni^{2+} have negligible absorbance at wavelengths tested in this study (200–400 nm). Nevertheless, the binding of Co^{2+} and Ni^{2+} to monolithic column was visualized by the color change in IDA column (pink for Co^{2+} and green for Ni^{2+}) and further confirmed by the specific color of the eluate due to the presence of each metal ion.

The effect of pH on the binding ability of Pb^{2+} to monolithic column was further investigated. After charging the column with Pb^{2+} at pH 5.4, the column was washed with buffer at pH 3.5 (Washing Buffer 2). It was confirmed that the amount of Pb^{2+} bound to the column was reduced with the decrease in pH (data not shown). This provides us a useful tool to increase the selection power by

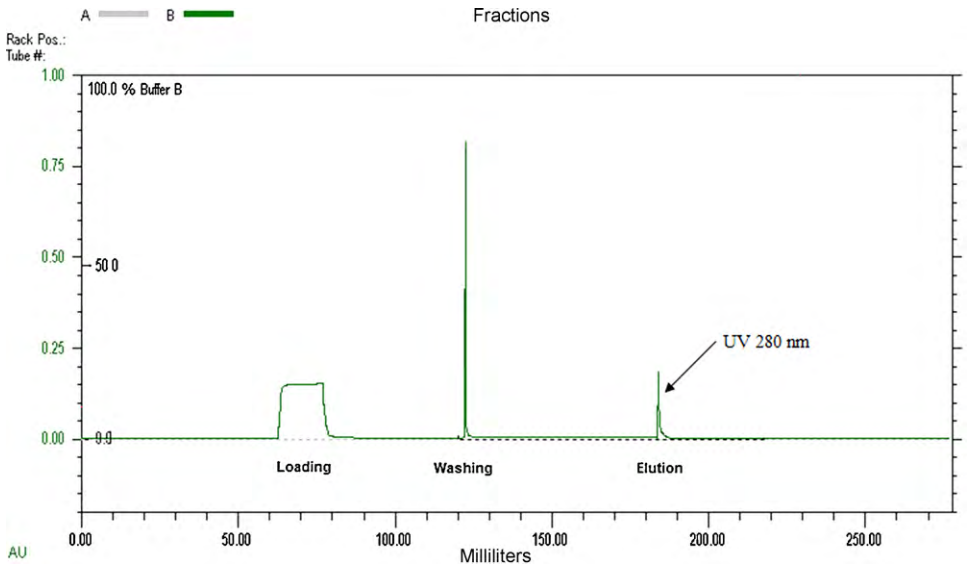

Fig. 1. Characterization of binding ability of Pb^{2+} to the monolithic column. 20 mL of metal ion solution (50 mM Pb^{2+}) was loaded to the monolithic column with 1 mL bed volume at a flow rate of 1 mL/min. The column was then washed with 60 mL Washing Buffer 1 to eliminate any unbound metal ion. 1 M HCl was used to elute the bound Pb^{2+}. Green line represents the UV absorbance at 280 nm. (For interpretation of the references to color in this figure legend, the reader is referred to the web version of the article.)

reducing the bound metal ions on the column in the following chromatographic biopanning experiments.

3.2. Chromatographic biopanning

The overall procedure for chromatographic biopanning is shown in Fig. 2. It includes pre-negative screening against IDA column only, main biopanning for Pb^{2+}, post-negative screening I against IDA column, followed by post-negative screening II for other metal ions (Cu^{2+}, Ni^{2+}, Co^{2+} and Fe^{3+}).

3.2.1. Pre-negative screening

Pre-negative screening was conducted by applying phage library to uncharged monolithic column in a total recycling mode to preclude phage particles exhibiting intrinsic affinity to IDA ligands or column matrix. The monolithic column claimed by BIA separations to have large diameter channels proved to successfully accommodate the phage particles (approximately 1 μm in length and 10 nm in diameter [12]). The M13 phage molecules with molecular weight of over 10,000 kDa [11,33] can be detected by UV at 280 nm. The flow rate was kept at 1 mL/min and 2 mL of flowthrough was collected after 25 min of total recycling of phage library suspension. 10 μL of the flowthrough was used for titering and the rest was used for phage amplification. The amplified phages were then titered and adjusted to a desired concentration (similar to the concentration of phage library applied, $\sim 1.8 \times 10^{13}$ pfu/mL) for the following positive screening. The number of phages applied for each biopanning step is shown in Table 1.

3.2.2. Main biopanning

Main biopanning was conducted for three rounds against Pb^{2+}-charged monolithic IDA column with monitoring of the time course of chromatographic biopanning (Fig. 3a–c) and phage number for each round of selection (Table 1). After loading phage samples obtained from the previous pre-negative selection, Washing Buffer 1 was used to eliminate any weakly bound phages. The elution was achieved by passing the column with 15 mL of 1 M HCl (Fig. 3a). The amplified phages were titered and the concentration was adjusted to $\sim 1.8 \times 10^{13}$ pfu/mL and used for the second round (Fig. 3b, Table 1). After two rounds of positive selection, phage molecules having relatively high affinity to Pb^{2+} were increased (Table 1). To facilitate the enrichment of high affinity phage binders, the selection power in the third round was increased by reducing the amount of Pb^{2+} bound to the column (Fig. 3c) by applying Washing Buffer 2 at pH 3.5 following the immobilization of Pb^{2+} at pH 5.4. The eluate was titered and the amplified eluted phage was used for the following negative selection processes.

3.2.3. Post-negative screening I

Since the diversity of phage binders recovered from the positive selection was greatly reduced (Table 1), the number of amplified phages loaded onto the column was reduced. Instead of 100 μL of phage sample used in the above selection processes, 10 μL of phage sample from the third round positive selection (with a concentration of $\sim 1.0 \times 10^{13}$ pfu/mL) was dissolved in 500 μL Equilibration Buffer and applied to uncharged monolithic column in a total recycling mode. The number of loaded phages was therefore decreased to $\sim 1.0 \times 10^{11}$. Post-negative screening I was conducted according to the protocols described for pre-negative screening except for the aforementioned loading sample volume adjustment. After three rounds of post-negative selection, phage concentration in eluate was significantly reduced below the detection limit (e.g. ~1 phage virion per 10 μL used in phage titration) (Table 1). This can also be reflected in the chromatograms where the absorbance signal due to the presence of phage particles was significantly decreased (data not shown). We therefore decided to stop post-negative selection process for uncharged column and proceeded to post-negative screening against various other metal ions.

3.2.4. Post-negative screening II

10 μL of amplified phage sample from the eluate of the third round of post-negative selection was dissolved in 500 μL Equilibration Buffer and applied to monolithic column (charged with different kinds of metal ions) in a total recycling mode. 2 mL of flowthrough was collected and amplified for next round selection (Table 1). 4–5 mL eluate was collected and titered. According to the number of phages in the eluate after each round of selection, three rounds of negative selection against Cu^{2+}, three rounds against Ni^{2+}, two rounds against Co^{2+} and one round against Fe^{3+} were conducted (data not shown).

After chromatographic biopanning, 60 phage clones from the last round of post-negative screening II were selected for phage

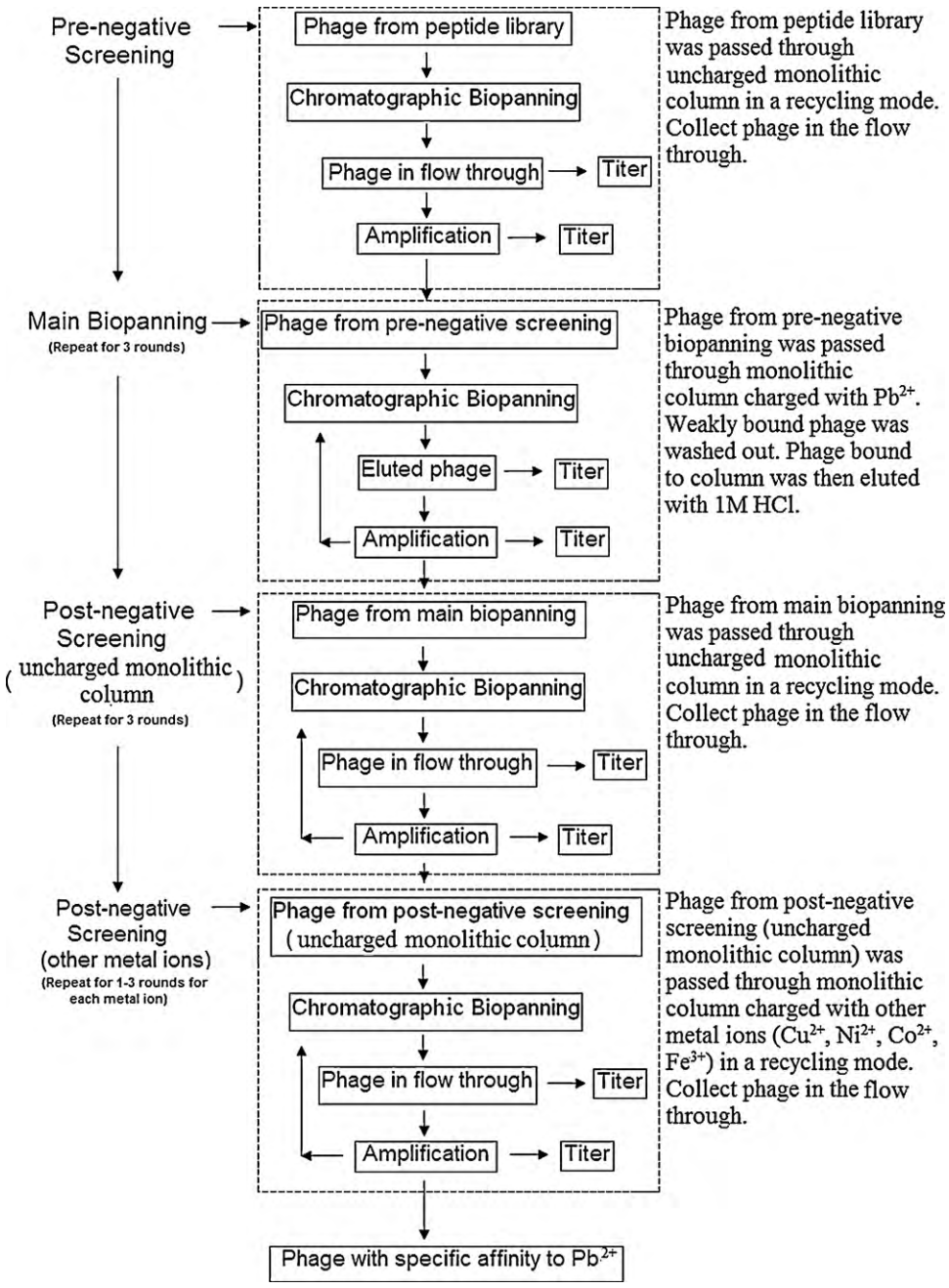

Fig. 2. Overview of chromatographic biopanning procedures including pre-negative screening against uncharged monolithic column, main biopanning against Pb^{2+}, post-negative screening against uncharged monolithic column, and post-negative screening for various other metal ions.

DNA sequencing, giving rise to 17 putative Pb^{2+}-specific peptide binders (Table 2). The specific affinity of these peptides to different metal ions was further tested by bead-based enzyme immunoassay.

3.3. Bead-based enzyme immunoassay (EIA) for selected phage peptides

The quantity of metal ions used to charge the IDA beads is a key factor affecting the EIA detection. If the amount of charged metal ion to beads is too low, this may lead to inadequate adsorption sites for phage binding, rendering a low signal to background noise ratio (i.e. the color development mediated by alkaline phosphatase conjugated to the secondary antibody cannot be clearly distinguished from the background). On the other hand, a significantly high background noise may arise if the amount of metal ions charged to beads is too much since the metal ions per se will also catalyze the color development reaction. The concentration of metal ions, therefore, must be optimized. In our experiment, 1 mL of 10 μM metal ion solution, which can provide sufficient ligands for phage binding while minimizing the background reaction catalyzed by metal ions alone, was found to be the suitable concentration to charge the IDA beads (200 μL SV).

The coupling efficiency of different metal ions to IDA beads at low pH was further investigated. 200 μL of IDA beads were incubated with 1 mL of 10 μM metal ion solution. After washing with water and Washing Buffer 3, the metal ions were eluted with 1 M HCl and the amount of bound metal ions analyzed by ICP-MS (Table 3). It was suggested that the binding efficiency of metal ions to IDA beads was significantly affected by pH, showing the strongest binding at near neutral pH (i.e. pH 7–8) [34]. Neverthe-

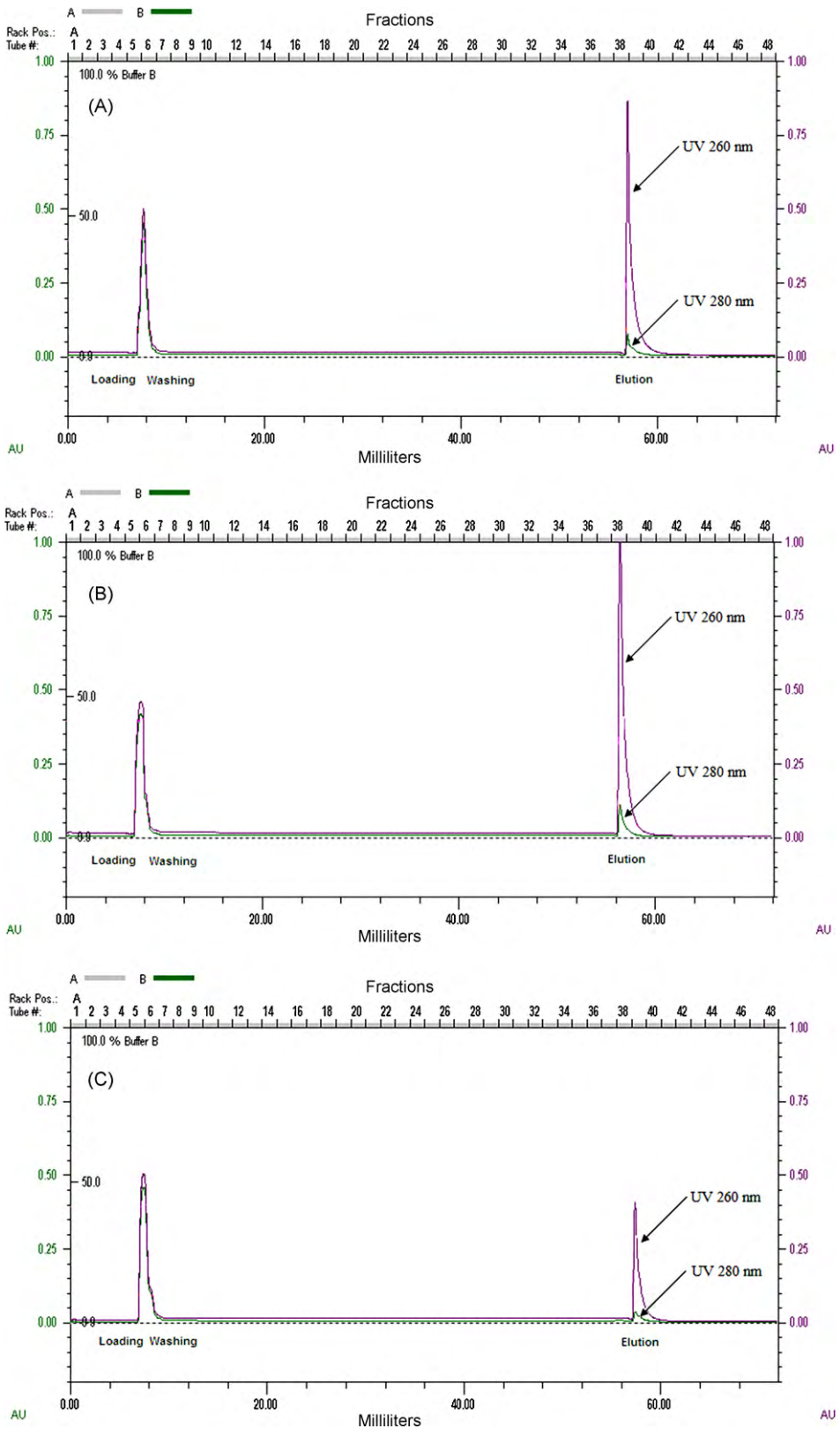

Fig. 3. Positive selection against Pb^{2+}. 100 μL of phage sample from pre-negative screening was dissolved in 900 μL Equilibration Buffer and loaded to the column pre-charged with Pb^{2+} at a flow rate of 0.5 mL/min. Washing Buffer 1 was used to extensively wash out any weakly bound phage at a flow rate of 2 mL/min. The elution was conducted by passing the column with 15 mL of 1 M HCl. Panel description: (a) first round of positive selection; (b) second round of positive selection and (c) third round of positive selection. The selection power was increased by reducing the amount of Pb^{2+} bound to the column. The eluate was titered and the amplified eluted phage was used for the following negative selection processes. Green and purple lines represent the UV absorbance at 280 and 260 nm, respectively. (For interpretation of the references to color in this figure legend, the reader is referred to the web version of the article.)

Table 1
The number of phages applied for each chromatographic biopanning step.

Library applied	~2.0×10^{12} virions				
		Figure	Flowthrough (total no.)	Eluate (total no.)	Amplified for next cycle (no. per mL)
Pre-negative selection	Round 1		~1.8×10^{12}	NA	~1.8×10^{13}
Main biopanning (Pb^{2+})	Round 1	3a	~1.5×10^{12}	~1.5×10^{8}	~1.9×10^{13}
	Round 2	3b	~2.0×10^{12}	~2.5×10^{8}	~2.1×10^{13}
	Round 3	3c	~1.6×10^{12}	~0.6×10^{8}	~1.0×10^{13}
Post-negative selection (uncharged monolithic column)	Round 1		~0.8×10^{11}	~0.6×10^{6}	~1.0×10^{13}
	Round 2		~0.9×10^{11}	~1.0×10^{4}	~1.0×10^{13}
	Round 3		~0.8×10^{11}	<0.8×10^{3}	~1.0×10^{13}
Post-negative selection (Cu^{2+})	Round 1		~1.2×10^{11}	~1.0×10^{4}	~1.3×10^{13}
	Round 2		~0.8×10^{11}	~1.0×10^{3}	~1.0×10^{13}
	Round 3		~0.7×10^{11}	<1.0×10^{3}	~1.0×10^{13}
Post-negative selection (Ni^{2+})	Round 1		~1.3×10^{11}	~0.5×10^{6}	~1.3×10^{13}
	Round 2		~1.4×10^{11}	~0.7×10^{4}	~1.6×10^{13}
	Round 3		~1.5×10^{11}	<1.0×10^{3}	~2.4×10^{13}
Post-negative selection (Co^{2+})	Round 1		~2.5×10^{11}	~0.7×10^{6}	~2.3×10^{13}
	Round 2		~2.8×10^{11}	<1.0×10^{3}	~1.9×10^{13}
Post-negative selection (Fe^{3+})	Round 1		~1.9×10^{11}	<1.0×10^{3}	~2.1×10^{13}

Table 2
Amino acid sequences of selected Pb^{2+} binding peptides and the analysis of Pb^{2+} binding peptide sequences based on amino acid property.

No.	Amino acid composition of selected peptide	Amino acid composition of selected peptide	Frequency of each sequence	Representation of each amino acid according to its corresponding property
1	Cys Lys Ser Leu Glu Tyr Ser Tyr Cys	C KSLEYSY C	18	bonaooo
2	Cys Lys Ser Pro Glu Asn Ser Tyr Cys	C KSPENSY C	6	bonapoo
3	Cys Thr Asn Thr Leu Ser Asn Asn Cys	C TNTLSNN C	5	oponopp
4	Cys Thr Asn Thr Leu Asn Tyr Asn Cys	C TNTLNYN C	2	oponpop
5	Cys Lys Ser Thr Glu Asn Ser Tyr Cys	C KSTENSY C	1	booapoo
6	Cys Lys Ser Pro Glu Asn Tyr Tyr Cys	C KSPENYY C	1	bonapoo
7	Cys Lys Ser Pro Glu Asn Tyr Asn Cys	C KSPENYN C	1	bonapop
8	Cys Lys Ser Leu Glu Asn Tyr Tyr Cys	C KSLENYY C	1	bonapoo
9	Cys Lys Ser Met Glu Asn Ser Tyr Cys	C KSMENSY C	1	bonapoo
10	Cys Lys Tyr Thr Glu Ser Tyr Asn Cys	C KYTESYN C	1	booaoop
11	Cys Lys Tyr Leu Glu Asn Ser Tyr Cys	C KYLENSY C	1	bonapoo
12	Cys Lys Ser Pro Glu Asn Ser Ser Cys	C KSPENSS C	1	bonapoo
13	Cys Asn Asn Thr Gln Ser Tyr Asn Cys	C NNTQSYN C	1	ppopoop
14	Cys Thr Thr Pro Gly Asn Tyr Asn Cys	C TTPGNYN C	1	oonnpop
15	Cys Lys Thr Arg Glu Asn Ser Tyr Cys	C KTRENSY C	1	bobapoo
16	Cys Lys Ser Thr Gln Asn Ser Asn Cys	C KSTQNSN C	1	booppop
17	Cys Lys Asn Thr Glu Asn Tyr Asn Cys	C KNTENYN C	1	bpoapop
Total			44	

o: OH containing (S, T, Y); n: Nonpolar (A, V, L, I, F, W, M, P, G); p: Polar, uncharged (C, N, Q); b: Basic, polar (K, R, H); a: Acidic, polar (D, E).

less, as demonstrated in Table 3, a fairly large amount of metal ions could be bound to IDA beads at pH 4, enabling the selection of specific peptide sequences at a relatively low pH value.

Fig. 4 illustrates the absorbance in the EIA assay for the screened peptides at a phage concentration of 10^{10} pfu/mL, reflecting the binding efficiency of these peptides to Pb^{2+}. Peptide sequences displayed on phage clones B1, B3, B4 and B5 show relatively strong binding affinity to Pb^{2+} compared to the other peptide sequences including those displayed on the phage library (column 16), and wild type phage (column 17). The following experiment further demonstrated the effect of phage concentration on the binding of the high affinity binders (i.e. B1, B3, B4 and B5) to Pb^{2+}. As shown in Fig. 5, the absorbance from binding of these phage particles to metal ions increases along with the increasing number of phages and reaches a plateau when phage number is higher than 10^{10} pfu, suggesting that the binding capacity provided by Pb^{2+} for phages is saturated. As dissociation constant (K_d) is defined as follows: K_d = [peptide] × [metal ion]/[peptide – metal ion complex], at peptide concentration corresponding to half maximal signal (i.e. $[peptide]_{1/2}$), one-half of the metal ions are free and the other one-half bound to peptide molecules. At this equilibrium condition (i.e. $[metal\ ion]_{1/2} = [peptide - metal\ ion\ complex]_{1/2}$), K_d is equivalent to $[peptide]_{1/2}$. The calculated K_d for B1, B3, B4 and B5 are presented in Table 4. Note that the K_d for B4 is the lower than B3, indicating tighter binding between phage peptide B4 and Pb^{2+}. Phage peptide B3 on the other hand has a higher capacity to bind Pb^{2+}, as shown in Figs. 4–6.

Cross-binding assay was next conducted to investigate the specificity of the high affinity Pb^{2+} binders to different metal ions.

Table 3
Characterization of the metal ion binding capacity of IDA beads for various metal ions at pH 4. Metal ion concentration was determined by ICP-MS.

Metal ion	Pb^{2+}	Ni^{2+}	Co^{2+}	Cu^{2+}	Fe^{3+}
Binding capacity (nmole per mL beads)	9.0	12.0	2.5	250.0	31.5

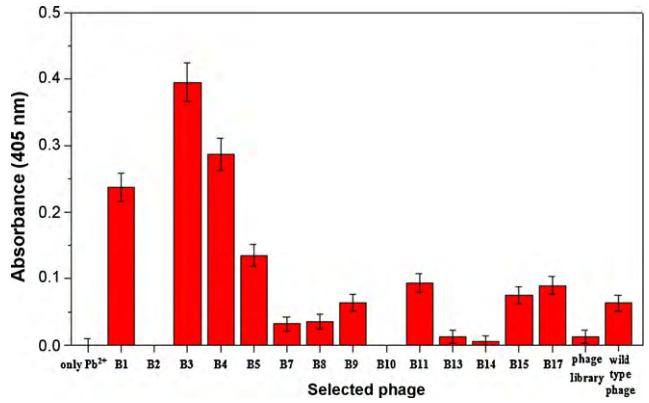

Fig. 4. Characterization of the binding affinity of selected phages to Pb^{2+}. The concentration of each phage was adjusted to $\sim 2 \times 10^{11}$ pfu/mL and 50 μL was applied for bead-based EIA as aforementioned (the total number of applied phages is $\sim 10^{10}$). The background absorbance caused by the presence of Pb^{2+} was subtracted from the absorbance produced by each phage binder.

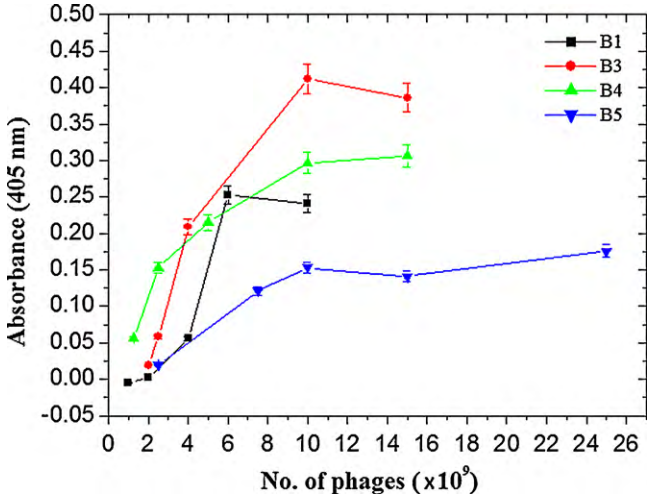

Fig. 5. Effect of phage concentration on the binding affinity to Pb^{2+}. Selected high affinity Pb^{2+} binding phages (B1, B3, B4, and B5) at different concentrations were incubated with Pb^{2+}-charged IDA beads. The background absorbance caused by the presence of Pb^{2+} was subtracted from the absorbance produced by each phage binder.

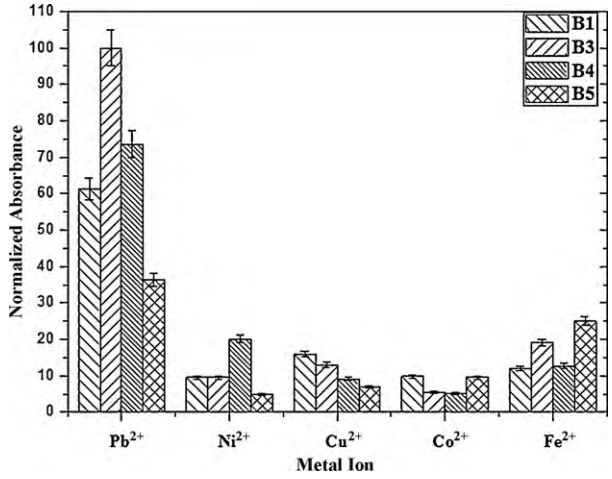

Fig. 6. Cross-binding assay for high affinity Pb^{2+} binders (B1, B3, B4 and B5) to different metal ions. Equivalent amount of different metal ions was used to charge IDA beads. After extensive washing, 10^{10} of each phage was applied. The background absorbance due to the presence of metal ions was subtracted from the absorbance produced by each phage binder. The absorbance by each phage binder was normalized with that for phage clone B3 binding to Pb^{2+} as 100% basis.

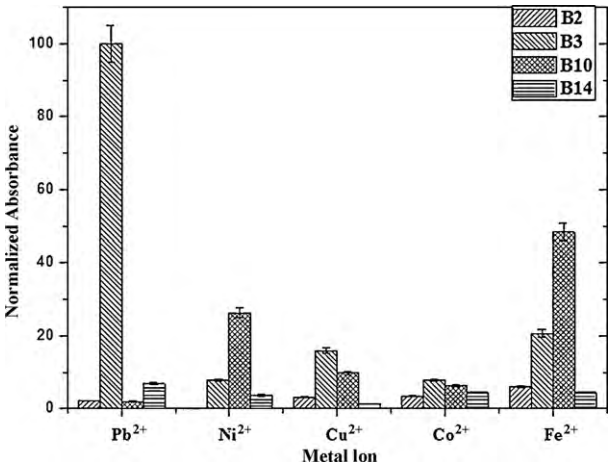

Fig. 7. Cross-binding assay for selected phage (B2, B3, B10, and B14) to different metal ions. The background absorbance due to the presence of metal ions was subtracted from the absorbance produced by each phage binder. The absorbance by each phage binder was normalized with that for phage clone B3 binding to Pb^{2+} as 100% basis.

Equivalent amount of different metal ions was used to charge IDA beads. After extensive washing, 10^{10} of each phage was incubated with the immobilized metal ions. The background absorbance caused by the metal ion catalyzed reaction was subtracted from the absorbance for each EIA reaction signal measured at 405 nm. As shown in Table 3, since the amount of each metal ion binding to IDA beads is different, the number of binding sites that these metal ions provide for the accommodation of phage particles also varied. This may affect the absorbance signals and hinder the comparison of binding efficiency of the same peptide sequence to different metal ions. Nevertheless, according to Table 3, all the metal ions tested (except Co^{2+}) show higher binding ability to IDA beads than Pb^{2+}. Hence, if the affinity between the phage and metal ion is similar, the binding of phage particles should be second lowest for Pb^{2+}-IDA. Any increase in phage particles bound to Pb^{2+} over other metal ions (except Co^{2+}) should directly indicate that the affinity for the phage is higher for Pb^{2+} (i.e. despite the lower amount of Pb^{2+} ligands, more phage molecules are bound).

As shown in Fig. 6, phage clone B3 exhibits the strongest and the most specific binding to Pb^{2+}. In order to investigate whether the phage clones with weak binding ability may have more specific binding to Pb^{2+}, in the control experiment, phage clones B9, B11, B14 and B15 which exhibited weak binding to Pb^{2+} were also tested for their cross-binding to different metal ions. These phage particles display relatively low binding affinities to all the metal ions tested including Pb^{2+} with significantly compromised specificity to Pb^{2+} (data not shown).

To highlight the differences in the binding affinity and specificity of a high affinity binder (e.g. B3) as compared with other low affinity binders, EIA was conducted for phage clones B2, B3, B10 and B14. According to Fig. 7, B3 shows the best relative binding affinity and specificity to Pb^{2+}, significantly departing from the binding behavior of B2, B10 or B14 which shows a negligible binding affinity

Table 4
Dissociation constants (K_d) of selected phage peptides (extracted from Fig. 5).

Phage peptide	K_d
B1	3.9×10^{-11} M
B3	3.3×10^{-11} M
B4	2.2×10^{-11} M
B5	4.3×10^{-11} M

or specificity to Pb^{2+}. Therefore, B3 is concluded to be the best Pb^{2+} binder with the highest relative binding affinity and specificity to the target.

Since metal binding peptides have many functions (e.g. affinity chromatography to purify proteins [35], bioremediation [36,37], and structural and catalytic roles in enzymes [38]), many studies on metal binding peptides have been conducted. For example, noble metals such as gold [39] and silver [40], heavy metals such as cadmium and mercury [36,37,39,41], and metals which are physiologically important, such as zinc [38] and aluminium [42], have been explored to identify metal ion cognitive peptide sequences. It should be noted that most of these studies were conducted at a neutral pH (~7.5) and that few studies applied phage display technique in a low pH (e.g. pH 5.4 and 3.5 as was demonstrated in our study). This is restricted mainly by the precipitation-prone feature of Pb^{2+} since Pb^{2+} is well-known to form complex with various kinds of anions (e.g. Cl^-, $SO_4{}^{2-}$). The precipitation of $Pb(OH)_2$ also causes difficulty in tracking free Pb^{2+} ions at pH higher than 5. Polyhistidine tags are the most well recognized peptide sequence exhibiting strong affinity to various types of metal ions (Cu^{2+}, Co^{2+}, Ni^{2+}, Zn^{2+} and Fe^{3+}). One or several histidine residues are also frequently found in peptides that show binding affinity to Zn^{2+} [38], Cd^{2+} [43], Ni^{2+} [44], and Cu^{2+} [45]. Our study is the first to utilize chromatographic biopanning combined with phage display technique at low pH to discover peptide sequences exhibiting specific affinity toward Pb^{2+}. A new pattern of peptide sequence was found which has high specific affinity to Pb^{2+} (Table 2). Phage clone B3 displaying ThrAsnThrLeuSerAsnAsn (TNTLSNN) heptapeptide on the viral surface gave the highest binding affinity and specificity to Pb^{2+}. It is interesting to note that histidine residue, often known to show high affinity at neutral pH to positively charged metal ions, is absent in B3. This may be due to the low pH screening condition conducive to protonation of lone pair electrons on the imidazole side chain of histidine hence weakening the binding affinity of histidine residue to metal ions. On the contrary, polar but uncharged residue (e.g. Asn) and OH-containing hydroxyl residues (e.g. Thr and Ser) are dominant in the Pb^{2+}-binding peptide B3 at low pH (in the 7 amino acid sequence, 3 of each Asn and hydroxyl residues are present). At the moment, it is unclear if B3 peptide binding to Pb^{2+} can be primarily attributed to the presence of a consensus sequence with patterned positioning of polar uncharged and/or hydroxyl amino acid residues. According to the previous studies to address underpinning mechanisms of peptide binding to various metal or metal oxide compounds, it seems that multiple factors (sequence, local structure, and context of peptide in conjunction with neighboring milieu) all interplay together in a complicated manner to account for peptide-target recognition [42,46,47]. The elucidation of molecular mechanism of B3 binding to Pb^{2+} will therefore require further independent study.

4. Conclusion

A peptide sequence B3 (TNTLSNN) was successfully found using a novel monolith-based chromatographic biopanning procedure and its high relative binding affinity and specificity to Pb^{2+} was confirmed. Monolith-based chromatographic biopanning procedure demonstrated in this study proves to be superior to the conventional biopanning procedures in many aspects. First, it enables the use of monolith matrix in the biopanning of target cognitive peptides displayed on the phage surface in an automated FPLC platform which would otherwise be cumbersome, time-inefficient and labor-intensive in the traditional protocols. Second, it facilitates screening of peptides with high affinity and specificity to a target by harnessing multi-stage adsorption/desorption equilibrium for efficient fractionation of binders from weak or non-binders which is rarely realized in the conventional biopanning procedures based on a single equilibrium stage batch adsorption, thereby significantly reducing the number of screening rounds required for enriching high affinity peptide binders. Finally, its operating strategy is highly flexible and conducive to being tailored to suit the purpose of screening, which is rarely expected in the traditional panning method. For example, chromatographic panning can take place in a total recycle mode for negative screening to maximize the efficiency of removing non-specific binders in order to selectively enrich highly specific binders to a target. For the same purpose, it is advantageous to run a positive screening round in a pass-through mode. Alternatively, if binders from the original library to a target are rare, positive screening step can be operated in a total recycle mode to provide more opportunities for peptide library members to interact with the target. With these merits, the demonstrated new monolith-based chromatographic biopanning procedure is likely to find wide applications in the screening of peptide binders to a broad range of target molecules.

Acknowledgement

This work was supported by Korea Institute of Environmental Science and Technology (KIEST, Grant no. 2008-10001-0029-0).

References

[1] D.G. McDonald, A.F. Grandt, Limestone – Lime Treatment of Acid Mine Drainage – Full Scale, 1981.
[2] B.J. Alloway, Heavy Metals in Soils, 2nd ed., Chapman and Hall, Glasgow, UK, 1995 (Chapters 6, 8, 9 and 11).
[3] R.C. Wilmoth, J.L. Kennedy, Industrial Environmental Research Laboratory, Removal of Trace Elements from Acid Mine Drainage, 1979.
[4] W. Wang, X. Zheng, J. Finck, Environ. Sci. Technol. 30 (1996) 2604.
[5] D.E. Salt, M. Blaylock, P.B.A. Nanda Kumar, V. Dushenkov, B.D. Ensley, I. Chet, I. Raskin, Nat. Biotechnol. 13 (1995) 468.
[6] V. Dushenkov, P.B.A. Nanda Kumar, H. Motto, I. Raskin, Environ. Sci. Technol. 29 (1995) 1239.
[7] S.S. Sidhu, Curr. Opin. Biotechnol. 11 (2000) 610.
[8] D.J. Rodi, L. Makowski, Curr. Opin. Biotechnol. 10 (1999) 87.
[9] D.R. Wilson, B.B. Finlay, Can. J. Microbiol. 44 (1998) 313.
[10] S.F. Parmley, G.P. Smith, Gene 73 (1988) 305.
[11] G.P. Smith, V.A. Petrenko, Chem. Rev. 97 (1997) 391.
[12] S.S. Sidhu, Biomol. Eng. 18 (2001) 57.
[13] A.V. Patwardhan, G.N. Goud, R.S. Pasquinelli, R.R. Koepsel, M.M. Ataai, Biotechnol. Technol. 12 (1998) 421.
[14] A. Maruška, O. Kornyšova, J. Chromatogr. A 1112 (2006) 319.
[15] M.A. Rostagno, M. Palma, C.G. Barroso, Anal. Chim. Acta 582 (2007) 243.
[16] G. Guiochon, J. Chromatogr. A 1168 (2007) 101.
[17] K.K. Unger, R. Skudas, M.M. Schulte, J. Chromatogr. A 1184 (2008) 393.
[18] J.M. Davis, D.J. Svendsgaard, Nature 329 (1987) 297.
[19] D. Sutoo, in: R.L. Isaacson, K.F. Jensen (Eds.), The Vulnerable Brain and Environmental Risks, vol. 3, Plenum Press, New York, 1994, p. 281.
[20] G. Erenberg, S.S. Rinsler, B.G. Fish, Pediatrics 54 (1974) 438.
[21] R. Nilsson, J. Water Res. 5 (1971) 51.
[22] R.V. Day, E.T. Lee, E.S. Hochuli, J. Ind. Wastes 20 (1974) 26.
[23] M. Nozaki, H. Hatotani, J. Water Res. I (1967) 167.
[24] C.F. Liebig, A.P. Vanselow Jr., H.D. Chapman, J. Soil Sci. 55 (1943) 371.
[25] T. Maruyama, S.A. Hannah, J.M. Cohen, J. Water Pollut. Contam. Fed. 47 (1975) 440.
[26] A.H. Nicholas, S.P.K. Stemberg, Int. J. Phytoremediation 10 (2008) 278.
[27] N.R. Axtell, S.P.K. Sternberg, K. Claussen, Bioresour. Technol. 89 (2003) 41.
[28] M. Mejáre, L. Bülow, Trends Biotechnol. 19 (2001) 67.
[29] P. Kotrba, L. Doleková, V. de Lorenzo, T. Ruml, Appl. Environ. Microbiol. 65 (1999) 1092.
[30] M. Pazirandeh, B.M. Wells, R.L. Ryan, Appl. Environ. Microbiol. 64 (1998) 4068.
[31] C. Sousa, A. Cebolla, V. de Lorenzo, Nat. Biotechnol. 14 (1996) 1017.
[32] C.H. Ward, D.A. Hlousek, T.A. Phillips, D.F. Lowe, Remediation of Firing Range Impact Berms, CRC Press, 2000.
[33] S. Cabilly, Mol. Biotechnol. 12 (1999) 143.
[34] E.K.M. Ueda, P.W. Gout, L.C. Morganti, J. Chromatogr. A 988 (2003) 1.
[35] R.R. Beitle, M.M. Ataai, Biotechnol. Prog. 9 (1993) 64.
[36] M. Satoh, E. Karaki, M. Kakehashi, E. Okazaki, T. Gotoh, Y. Oyama, J. Phycol. 35 (1999) 989.
[37] T.M. DeSilva, G. Veglia, F. Porcelli, A.M. Prantner, S.J. Opella, Biopolymers 64 (2002) 189.
[38] T. Matsubara, Y. Hiura, O. Kawahito, M. Yasuzawa, K. Kawashiro, FEBS Lett. 555 (2003) 317.
[39] S. Brown, Nat. Biotechnol. 15 (1997) 269.

[40] R.R. Naik, S.J. Stringer, G. Agarwal, S.E. Jones, M.O. Stone, Nat. Mater. 1 (2002) 169.
[41] M. Matzapetakis, B.T. Farrer, T.-C. Weng, L. Hemmingsen, J.E. Penner-Hahn, V.L. Pecoraro, J. Am. Chem. Soc. 124 (2002) 8042.
[42] R. Zuo, D. Örnek, T.K. Wood, Appl. Microbiol. Biotechnol. 68 (2005) 505.
[43] P. Kotrba, L. Delečková, V. De Lorenzo, T. Ruml, Appl. Environ. Microbiol. 65 (1999) 1092.
[44] P. Samuelson, H. Wernérus, M. Svedberg, S. Ståhl, Appl. Environ. Microbiol. 66 (2000) 1243.
[45] A.V. Patwardhan, G.N. Goud, R.R. Koepsel, M.M. Ataai, J. Chromatogr. A 787 (1997) 91.
[46] C.K. Thai, H. Dai, M.S.R. Sastry, M. Sarikaya, D.T. Schwartz, F. Baneyx, Biotechnol. Bioeng. 87 (2004) 129.
[47] H. Chen, X. Su, K.G. Neoh, W.S. Choe, Anal. Chem. 78 (2006) 4872.